Role of Cu^+ Association on the Formamide → Formamidic Acid → (Aminohydroxy)carbene Isomerizations in the Gas Phase

A. Luna, J.-P. Morizur, and J. Tortajada*

Laboratoire de Chimie Organique Structurale, Université Pierre et Marie Curie, Boite 45, CNRS UMR 172, 4 Place Jussieu, 75252 Paris Cedex 02, France

M. Alcamí, O. Mó, and M. Yáñez*

Departamento de Química, C-9, Universidad Autónoma de Madrid, Cantoblanco, 28049-Madrid, Spain

Received: January 5, 1998; In Final Form: March 13, 1998

The structures, relative stabilities, and bonding characteristics of complexes of formamide, formamidic acid, and (aminohydroxy)carbene with Cu^+ have been investigated through the use of high-level density functional theory (DFT) calculations. Geometries were optimized at the B3LYP/6-311G(d,p) level, while the final energies were obtained using a 6-311+G(2df,2p) basis set expansion. Contrarily to what happens upon association with alkali metal cations, the energy gaps between formamide and its two isomers decrease significantly upon Cu^+ association, because formamidic acid and (aminohydroxy)carbene exhibit higher Cu^+ binding energies than formamide. This behavior is similar to the one exhibited in the protonation processes, indicating that the neutral−Cu^+ interactions have a sizable covalent character. Nevertheless, the isomerization processes among the systems studied (formamide, formamidic acid, (aminohydroxy)carbene) are not catalized by Cu^+ ions, since in general the hydrogen transfers involved in such isomerization processes result in a weakening of the interaction between the neutral and the metal cation. The only exception to this general behavior corresponds to the isomerization between the nitrogen attached formamide complex and the corresponding enolic species, because in this particular case the hydrogen shift enhances the ion−neutral interaction.

Introduction

Formamide is the simplest amide containing a prototype HNC═O peptide linkage, and, for this reason, it is frequently used as a model for understanding proton exchange processes in peptides and proteins[1] or the hydrolysis of peptide bonds[2] in living systems. On the other hand formamide has, in principle, two different basic centers, the carbonyl oxygen and the amino nitrogen, which can compete in gas-phase reactions with different reference acids. Furthermore, formamide (**1**) has two tautomers, namely, formamidic acid (**2**), which corresponds to the enol form, and (aminohydroxy)carbene (**3**), and both have been generated recently in the gas phase by one-electron reduction of the corresponding radical cations.[3] The existence of these tautomers can be of paramount importance in rationalizing the gas-phase reactivity of formamide, since the observed chemical reactions, for instance the loss of water, involve necessarily the formation of these tautomers as a primary mechanism. The possibility of producing the enolic and the carbenic tautomers of formamide in the gas phase increases the interest on the isomerization processes which connect the three stable species, along with some *ab initio* molecular orbital studies that have been devoted to estimating the corresponding isomerization barriers.[4−8] The most accurate G2 estimates[8] for the **1** → **2**, **1** → **3**, and **2** → **3** isomerization barriers (46.4, 72.5, and 83.4 kcal/mol, respectively) showed that these isomerizations involve high-energy barriers. In the same study[8] it was also shown that association with different metal monocations, namely, Li^+, Na^+, Mg^+, and Al^+, leads to an increase of the isomerization barriers, as a result of a significant change in the ion−dipole interactions which are dominant in these kinds of complexes, where the ion−molecule interactions are essentially electrostatic.

The aim of this paper is to investigate whether these isomerization processes can be catalized by association with closed shell transition metal monocations such as Cu^+ where the ion−molecule interactions have a sizably large covalent character.

We have recently started a systematic investigation[9−11] on the interactions between Cu^+ and simple molecules that can be considered as suitable models of more complex biochemical species. It is also worth mentioning that a considerable effort has been devoted recently to investigate the interactions between Cu^+ and molecules of biochemical interest (such as α-amino acids[12−14]), since Cu^+ reactions play an important role in biological media.[13,15] In this paper we shall address the subject of the possible catalytic effect of Cu^+ on the isomerization processes between formamide and its enolic and carbenic forms, through the use of density functional theory calculations. It is nowadays well-established that G2-type[16] calculations perform very well when an accurate description of the energetics of the different equilibrium structures of the potential energy surface and the transient species connecting them is required. Unfortunately, these kinds of calculations are very expensive for systems as large as formamide−Cu^+ complexes. A reasonably good alternative is the use of density functional theory (DFT) methods together with flexible enough basis sets. Calculations of this type have been shown[17−19] to provide proton affinities in close agreement with both the G2 and the experimental values. A similar performance has been found[9] when dealing with Cu^+ complexes involving sp, sp^2, and sp^3 nitrogen containing model compounds, namely, NH_3, NH_2CH_3, $NHCH_2$,

S1089-5639(98)00629-X CCC: $15.00
Published on Web 05/19/1998

and HCN. Also recently we have applied[10] this theoretical scheme to propose plausible mechanisms which can explain the most outstanding experimental features of the gas-phase reactions[10] between guanidine and Cu^+.

Computational Details

The geometries of the different species under consideration have been optimized using the hybrid density functional B3LYP method, i.e., Becke's three parameter nonlocal hybrid exchange potential[20] with the nonlocal correlation functional of Lee, Yang, and Parr.[21] This approach has been shown[22] to yield reliable geometries for a wide variety of systems. Geometry optimizations were performed using the all electron (14s9p5d/9s5p3d) basis of Watchers−Hay[23] for Cu, supplemented with one set of *f* polarization functions and the 6-311G(d,p) basis set for the remaining atoms of the system. The harmonic vibrational frequencies of the different stationary points of the potential energy surface (PES) have been calculated at this level of theory in order to identify the local minima and the transition states (TSs), as well as to estimate the corresponding zero point energies.

As mentioned above, we have shown that association energies for Cu^+ complexes obtained at the DFT/6-311+G(2df,2p) level are in reasonably good agreement with those estimated in the framework of the G2 theory,[16] where a 6-311+G(3df,2p) basis is the largest basis set expansion used. At this point there are two facts that must be clarified. Although for the sake of simplicity we maintain the nomenclature "6-311+G(2df,2p)" for all of the atoms, it must be kept in mind that for Cu^+ it corresponds to the (14s9p5d/9s5p3d) Watchers−Hay's basis supplemented with a set of (1s2p1d) diffuse components and with two sets of *f* functions (rather than *d* functions) and one set of *g* functions (rather than *f* functions) as the polarization basis. In all of these supplementary functions the coefficients are the standard ones implemented in the Gaussian 94 series of programs.[24] It should be noted that the basis set employed in these DFT calculations differs from that used in the G2 formalism in the number of sets of *d* (*f* for Cu) polarization functions included on the heavy atoms. We have tested,[9] by taking the Cu^+-NH_3 complexes as a suitable benchmark case, that the binding energies so obtained do not differ significantly from those calculated with the larger basis set, while the time of calculation is considerably reduced. Hence, the final energies of the different species under study were obtained in DFT/6-311+G(2df,2p) single point calculations at the aforementioned DFT optimized geometries.

To investigate the bonding features of the complexes under consideration, we used the atoms in molecules (AIM) theory of Bader.[25] We have located the bond critical points (i.e. points where the electron density function, $\rho(\mathbf{r})$, is minimum along the bond path and maximum in the other two directions), because the values of the charge density and its Laplacian at these critical points give useful information regarding the strength of the linkages. The Laplacian of the density, $\nabla^2\rho(\mathbf{r})$, as it has been shown in the literature,[25] identifies regions of the space wherein the electronic charge is locally depleted ($\nabla^2\rho > 0$) or concentrated ($\nabla^2\rho < 0$). The former situation is typically associated with interactions between closed shell systems (ionic bonds, hydrogen bonds, and van der Waals molecules), while the latter characterizes covalent bonds. There are, however, significant exceptions, mainly when the atoms involved in the bond are very electronegative. In these cases the so-called energy density,[26] $H(\mathbf{r})$, is a more reliable index. Negative values of the energy density indicate that a stabilizing charge concentration takes place in the bonding region, a situation which is typically associated with covalent bonds.

All calculations have been carried out using the Gaussian 94 series of programs.[24] The AIM analysis was performed using the AIMPAC series of programs.[27]

Results and Discussion

Structures and Bonding. In our theoretical survey we have optimized the geometries of all of the possible conformers of each species. In this respect it must be mentioned, for instance, that formamidic acid (**2**) and (aminohydroxy)carbene (**3**) have four and two different conformers, respectively. For the sake of simplicity, in what follows, we shall refer exclusively to the most stable one. As far as the Cu^+ complexes are concerned, we have considered the attachment of Cu^+ to all possible basic centers of the neutral species. This is of a particular relevance because, as we shall show later, the direct isomerization mechanisms between formamide−Cu^+ complexes and formamidic acid−Cu^+ or (aminohydroxy)carbene−Cu^+ species do not lead necessarily to the most stable isomer. Again, we will discuss in detail only the most stable conformer in each case. The corresponding B3LYP/6-311G(d,p) optimized geometries are given in Figure 1. This figure also includes the optimized geometries of the transient species involved in the isomerizations between the different neutral and cationic local minima. Their total energies are summarized in Table 1.

The B3LYP/6-311G(d,p) optimized geometries for the three neutrals do not differ appreciably from the MP2/6-31G(d) ones reported before in the literature.[8] Regarding the corresponding Cu^+ complexes, it is worth noting that, as we have previously shown in a recent paper,[11] the most stable formamide−Cu^+ complex **1OCu** corresponds to the oxygen adduct, the N adduct **1NCu** lying 20.9 kcal/mol higher in energy. In contrast, **2** behaves as a nitrogen base, with the oxygen attached species **2OCu** lying 27.3 kcal/mol higher in energy than the nitrogen attached species **2NCu**. Compound **3** behaves as a carbon base to yield **3CCu** as the most stable complex. The corresponding oxygen adduct **3OCu** lies 41.3 kcal/mol above **3CCu**. Our results show that no stable complex exists with the Cu^+ attached to the amino group of structure **3** since it collapses, without activation barrier, to the carbon attached species **3CCu**. Similarly to what has been found previously for guanidine−Cu^+ systems,[10] no chelated structures with the metal cation bridging between two basic centers were found to be stable. This was not the case for complexes between formamidic acid and other metal cations such as Li^+, where the metal interacts simultaneously with the nitrogen and the oxygen atoms.[8] Similar bridging structures have been reported for complexes between alkali metal cations and azoles,[28] azines,[29] and different DNA and RNA nucleobases.[30] As we shall discuss later, this noticeable difference is due to the different nature of the ion−neutral interactions, which in the case of the Cu^+ have a significant covalent character, while for alkali metal cations they are essentially electrostatic.[28,29]

Cu^+ association imparts a sizable stabilization of both **2** and **3** with respect to **1**. The relative energies shown in Table 1 indicate that, at the highest level of theory considered in this work, **1** is predicted to be 13.2 and 38.4 kcal/mol more stable than its isomers **2** and **3**, respectively, in good agreement with previous theoretical estimations[8] at the G2 level of theory. These energy gaps reduce to 7.1 and 16.4 kcal/mol, respectively, when the corresponding Cu^+ complexes are considered. This behavior is opposite to that found[8] upon association with other metal monocations such as Li^+, Na^+, Mg^+, and Al^+, where an increase of the energy gaps is found upon metal cationization.

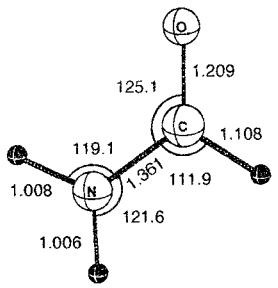

1

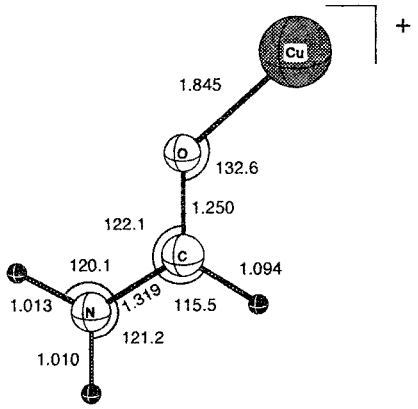

1OCu

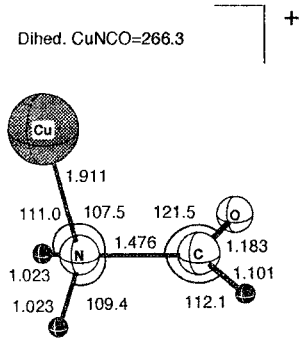

1NCu

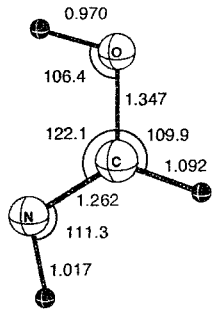

2

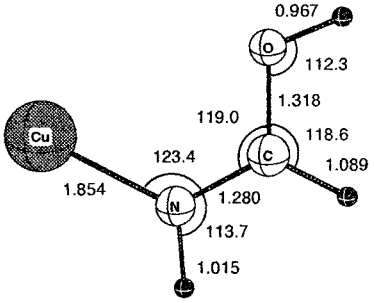

2NCu

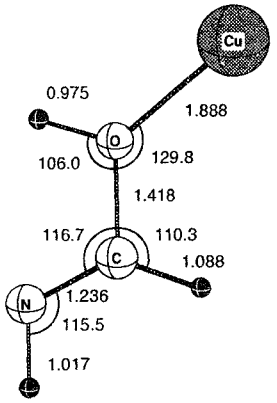

2OCu

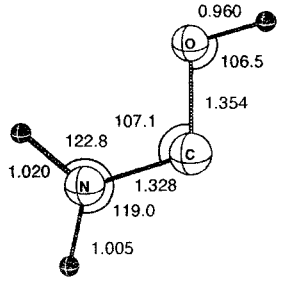

3

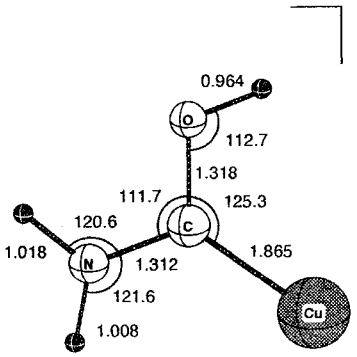

3CCu

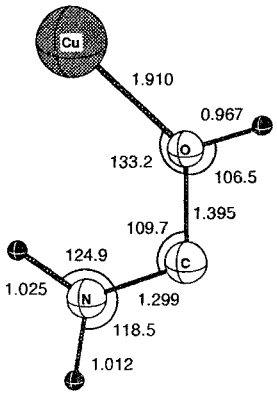

3OCu

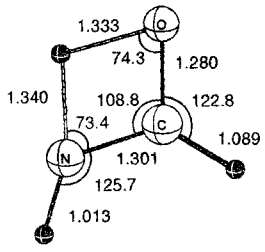

TS12

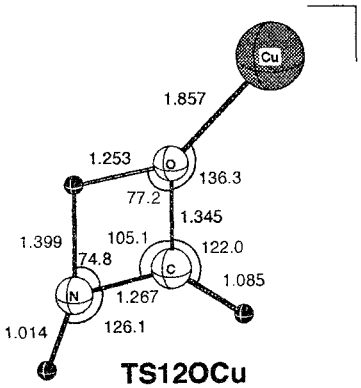

TS12OCu

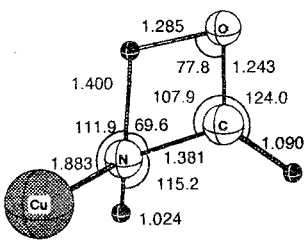

TS12NCu

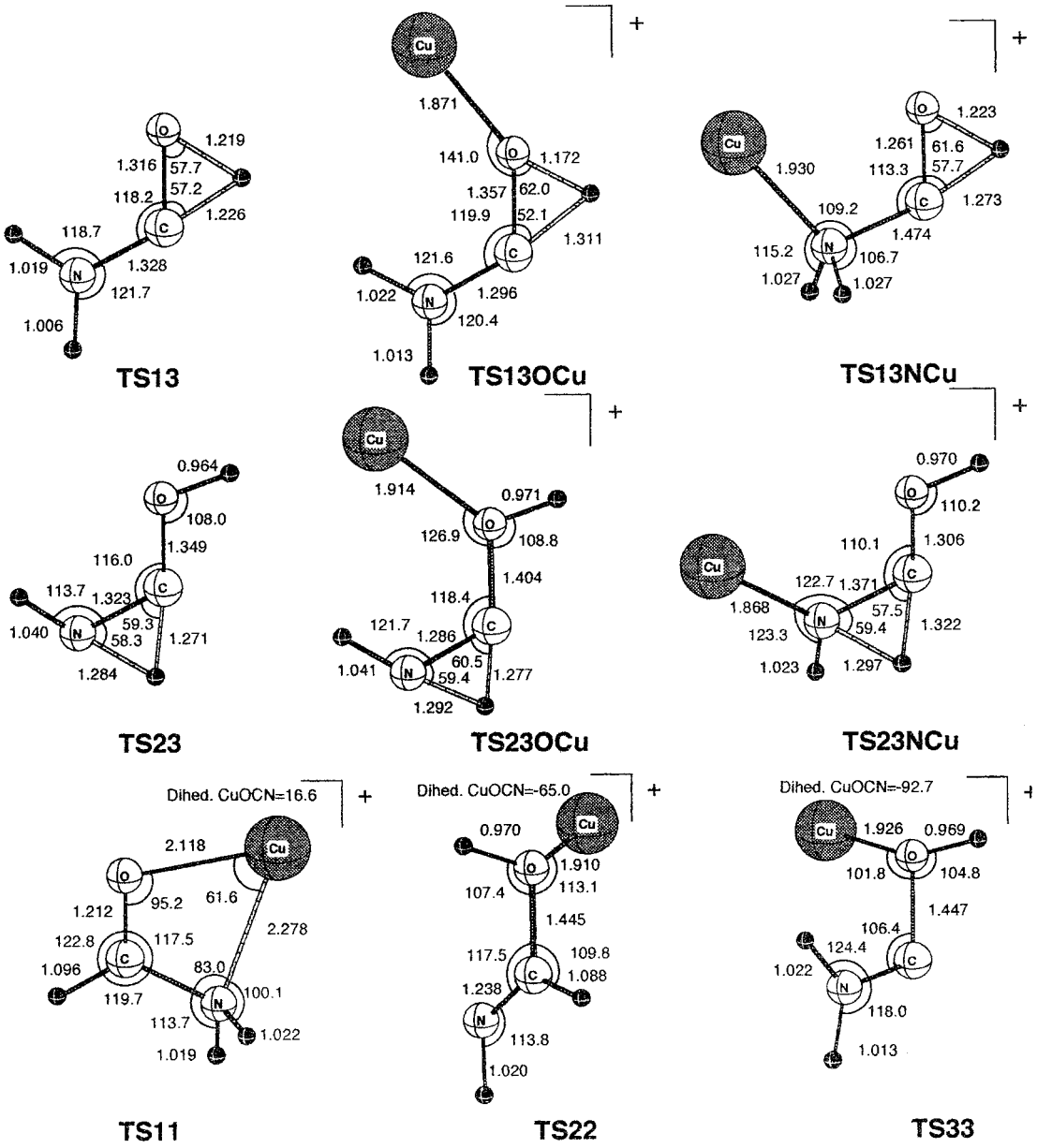

Figure 1. B3LYP/6-311G(d,p) optimized geometries of the stationary points associated with the PES of the formamide−Cu^+ → formamidic acid−Cu^+ → (aminohydroxy)carbene−Cu^+ isomerization processes. The optimized geometries of the corresponding neutrals are also included for the sake of comparison. Bond lengths in angstroms and bond angles in degrees.

This quite different behavior can be understood if one takes into account that in the latter cases the metal cation−neutral interactions are essentially electrostatic. Therefore, since both **2** and **3** have a smaller dipole moment than **1**, it is reasonable to expect the complexes formed by **2** and **3** to be less stable than those formed by **1**. In contrast, Cu^+−neutral interactions have a noticeable covalent character, which is reflected in the characteristics of the electron charge densities as well as on the large distortions caused in the geometry of the neutral. The AIM analyses show (see Table 2) that the charge densities at the N−Cu, O−Cu, and C−Cu bond critical points (bcps) are almost 1 order of magnitude larger than the typical values (0.012−0.038) found in ionic linkages.[8] Furthermore, the values of the corresponding energy densities are always negative, indicating that a stabilizing charge concentration within the bonding region, typically associated with covalent bonds, takes place. An inspection of the bonding MOs of these complexes shows that, as it has been found for other Cu^+ complexes,[9,10] the Cu uses sd hybrids to form bonding molecular orbitals with the lone-pair orbital of the base. As shown in ref 10 this interaction can be classified as a dative bond, so that Cu^+ constitutes an intermediate case between H^+ which yields strongly covalent bonds and alkali metal cations, which yield almost purely ionic interactions.

This is consistent with the significant geometrical distortions found upon Cu^+ association. As illustrated in Figure 1, attachment of Cu^+ to the carbon atom of **3** leading to **3CCu** produces a sizable shortening of both the C−N and C−O bonds. Consistently the charge densities at the corresponding bcps increase, and the energy densities become more negative. In comparison, the attachment of Cu^+ to the nitrogen atom of **2** to yield **2NCu** results in a significant lengthening of the C−N bond, while the C−O linkage becomes shorter. Again, these geometrical changes are consistent with the changes found in charge and energy densities evaluated at the corresponding bcps. As shown in Table 2, the charge density at the C−N bcp decreases and the energy density becomes less negative, while the opposite effects are found for the C−O bond. These changes

TABLE 1: Total Energies, ZPE (hartrees), and Relative Energies (kcal/mol) of the Stationary Points under Study at the B3LYP/6-311+G(2df,2p)//B3LYP/6-311G(d,p) Level. Cu^+ and H^+ Binding Energies, BE (kcal/mol), Are Also Included

system	absolute E	ZPE	E_{rel} (E_{rel} + ZPE)	BE Cu^+/H^+
1	−169.964 28	0.04531	0.0 (0.0)	56.2/197.1
2	−169.944 08	0.04614	12.7 (13.2)	62.4/210.3
3	−169.903 39	0.04570	38.2 (38.4)	78.3/235.5
guanidine	−205.458 26[a]	0.07598[a]		77.9/235.7[b,c]
	−205.029 41[b]			
NH_3	−56.586 39	0.03430		56.2/201.8
CH_3NH_2	−95.899 68	0.06382		59.8/213.0
CH_2NH	−94.668 31	0.03980		59.3/206.4
TS12	−169.887 51	0.04041	48.2 (45.1)	
TS13	−169.843 17	0.03935	76.0 (72.2)	
TS23	−169.823 53	0.03948	88.3 (84.7)	
1OCu	−1810.233 51	0.04825	0.0 (0.0)	
1NCu	−1810.200 18	0.04817	20.9 (20.9)	
2NCu	−1810.222 77	0.04876	6.7 (7.1)	
2OCu	−1810.177 08	0.04668	35.4 (34.4)	
3CCu	−1810.207 94	0.04875	16.0 (16.4)	
3OCu	−1810.140 06	0.04668	58.6 (57.7)	
TS12OCu	−1810.142 91	0.04220	56.9 (53.1)	
TS13OCu	−1810.098 00	0.04079	85.0 (80.3)	
TS23OCu	−1810.056 18	0.03954	111.3 (105.8)	
TS12NCu	−1810.136 18	0.04280	63.9 (60.5)	
TS13NCu	−1810.073 78	0.04104	100.2 (95.7)	
TS23NCu	−1810.084 43	0.04307	93.5 (90.3)	
TS22	−1810.169 98	0.04628	39.9 (38.6)	
TS33	−1810.134 04	0.04655	62.4 (61.3)	
$\mathbf{1H}^{+}$[d]	−170.292 69	0.05967		
NH_4^+	−56.923 11	0.04947		
CH_3-NH_3^+	−96.254 42	0.07916		
CH_2-NH_2^+	−95.011 49	0.05409		
guanidine−H^+	−205.401 13[b]			
guanidine−Cu^+	−1845.760 35[a]	0.07720[a]		
Cu^+	−1640.176 69[a]			

[a] Taken from ref 10. [b] G2 values taken from ref 17. [c] G2 value including thermal corrections. [d] It should be noted that species **1**−**3** yield a common cation, $\mathbf{1H}^+$, upon protonation.

TABLE 2: Charge Densities (ρ), Laplacian of the Charge Densities ($\nabla^2\rho$), and Energy Densities (H(r**)) Evaluated at the Corresponding Bond Critical Points (All Values in au)**

		CO	CN	CuN	CuC
2	ρ	0.299	0.401		
	$\nabla^2\rho$	−0.417	−1.137		
	H(**r**)	−0.433	−0.631		
2NCu	ρ	0.319	0.383	0.122	
	$\nabla^2\rho$	−0.369	−1.082	0.546	
	H(**r**)	−0.476	−0.863	−0.035	
3	ρ	0.286	0.333		
	$\nabla^2\rho$	−0.245	−0.797		
	H(**r**)	−0.408	−0.498		
3CCu	ρ	0.317	0.353		0.134
	$\nabla^2\rho$	−0.334	−0.952		0.362
	H(**r**)	−0.474	−0.532		−0.054

in the bonding characteristics affect also the vibrational frequencies, which are given as Supporting Information. Concerning to stretching-type frequencies, the association of Cu^+ to the carbon atom of (aminohydroxy)carbene implies a large blue shifting of the C−N (from 1425 to 1512 cm^{-1}) and C−O (from 1293 to 1395 cm^{-1}) stretching modes. Cu^+ association to the nitrogen atom of formamidic acid leads to a red shifting of the C−N stretch (from 1735 to 1726 cm^{-1}), while the C−O stretching frequency increases slightly (from 1332 to 1348 cm^{-1}). This different behavior can be easily explained by using arguments similar to those given by Alcamí et al.[31] to explain the strong charge redistributions which take place in protonation processes. The attachment of Cu^+ to the atom X of the base implies a significant charge transfer from the latter into the internuclear region to form a new X−Cu covalent linkage. This results in an enhancement of the electronegativity of X, which causes a drastic reorganization of the electron charge density of the system which depends on the relative electronegativity of X with respect to the atoms directly attached to it. For **2** the basic center (N) is more electronegative than the atom attached to it (C). In comparison, in **3** the basic center (C) is less electronegative than the atoms bonded to it (N and O). Hence, in the former case, the nitrogen atom recovers part of the charge which has been transferred into the N−Cu bonding region by depopulating the C−N bond, which accordingly becomes longer and weaker. This is not possible in the latter case, where the atoms attached to the basic center are very electronegative. However, since the C atom has an enhanced electronegativity it polarizes the charge around the atoms bonded to it into the corresponding bonding regions. As a consequence the bonds become reinforced and shorter.

Finally it should be mentioned that the attachment of Cu^+ to the nitrogen atom of the most stable conformer of **2** induces an internal rotation of the OH group to avoid the strong repulsive interaction between the positively charged Cu atom and the H atom. Thus, the **2NCu** complex can be viewed as the interaction between Cu^+ and the neutral conformer which has the hydroxyl hydrogen trans with respect to the imino group and which lies 6.3 kcal/mol above the global minimum.

The fact that the energy gaps between formamidic acid−Cu^+ and (aminohydroxy)carbene−Cu^+ complexes with regard to formamide−Cu^+ complexes are much smaller than those found between the corresponding neutral species indicates that both isomers **2** and **3** are more basic than **1** with respect to Cu^+. Quite importantly a similar enhanced basicity was reported in the literature with respect to proton attachment processes. It must be noted, however, that at the same level of theory, formamidic acid is predicted to have a proton affinity (PA) 18.1 kcal/mol greater than formamide (see Table 1), while its Cu^+ binding energy is only 11.1 kcal/mol greater than that of formamide. Similarly (aminohydroxy)carbene has a PA which is 38.4 kcal/mol higher than that of formamide, while its Cu^+ binding energy is only 22.1 kcal/mol higher. This confirms that Cu^+ association resembles closely proton association. Due to this analogy we thought it of interest to investigate whether there exists some direct relationship between proton affinities and Cu^+ binding energies. For this purpose we have chosen a series of bases whose Cu^+ binding energies have been estimated[9,10] at a level of accuracy analogous to the one employed in this work. For the sake of consistency the proton affinities of these bases were calculated using the same theoretical (B3LYP/6-311+G(2df,2p)) scheme as the one used to evaluate the corresponding Cu^+ binding energies (see Table 1). As illustrated in Figure 2, there is a reasonably good linear correlation between both sets of values, which indicates that relative Cu^+ binding energies are about 1.6 times smaller than relative proton affinities.

Isomerization Processes. The energy surfaces associated with the formamide−Cu^+ → formamidic acid−Cu^+ isomerization are shown schematically in Figure 3. For the sake of a better comparison we have included in the same figure the relevant information regarding the same isomerization process involving the neutral species. It can be observed, however, that when the metal cation is bonded to the oxygen atom of formamide, this 1,3H transfer, through the transient species **TS12OCu**, does not yield the most stable formamidic acid−Cu^+ complex **2NCu**, where the metal cation is attached to the

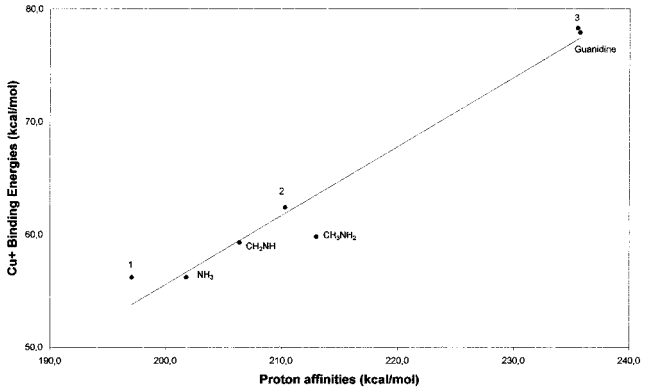

Figure 2. Linear correlation between Cu^+ binding energies and proton affinities for different bases. Values calculated at the B3LYP/6-311+G-(2df,2p) level. The correlated line obeys the following equation: BE-$(Cu^+) = 0.612$ PA $- 66.9$ kcal/mol, with a correlation coefficient $r = 0.98$.

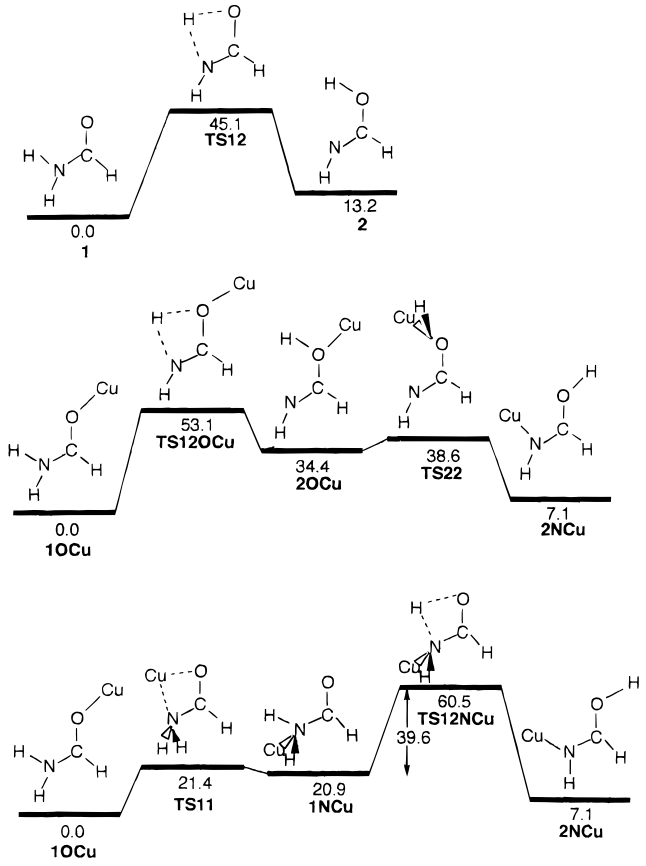

Figure 3. Schematic representation of the PES's associated with the formamide$-Cu^+ \rightarrow$ formamidic acid$-Cu^+$ isomerizations. The isomerization between the neutrals is also given for the sake of comparison. Relative energies are in kilocalories per mole.

nitrogen, but the isomer **2OCu**. A further internal rotation of the HOCu fragment of species **2OCu** leads, through the transition state species **TS22**, to the global minimum **2NCu**. Since the barrier involved in this second process is considerably smaller than the first one, the aforementioned 1,3H transfer is the limiting step.

Although, as mentioned above, in gas-phase reactions between Cu^+ and formamide the attachment takes place preferentially at the oxygen atom, it is also true that the isomerization barrier connecting the oxygen attached (**1OCu**) and the nitrogen attached species (**1NCu**), through the transition state **TS11**, is not very high. Taking into account that this energy barrier (see Figure 3) is much lower than those involved in the **1** $\rightarrow$ **2** $\rightarrow$ **3** isomerization processes, in what follows we will also considered the possible isomerization pathways which originate in the nitrogen attached complex **1NCu**.

As illustrated in Figure 3, once species **1NCu** is formed, a 1,3H transfer through the transient species **TS12NCu**, followed by an internal rotation of the OH group (not shown in the figure), would lead to the most stable formamidic acid$-Cu^+$ complex, **2NCu**.

The second important feature of Figure 3 is that formamide $\rightarrow$ formamidic acid isomerization is catalized by Cu^+ only if the metal cation is attached to the amino group, i.e., if the starting point is the **1NCu** complex rather than the global minimum **1OCu**. This finding can be understood if one takes into account that the transition state **TS12** is a poorer oxygen base but a stronger nitrogen base than formamide. Actually, in **TS12** one of the lone pairs of the oxygen atom is partially engaged in the O$-$H linkage which is being formed, and therefore its intrinsic basicity decreases. The situation is just the opposite when the amino group is considered, since one of the hydrogen atoms initially bonded to the nitrogen is moving away, enhancing the nitrogen intrinsic basicity. Figure 3 shows that the activation barrier which connects the oxygen (**1OCu**) and the nitrogen (**1NCu**) attached species of formamide was estimated[11] to be 21.4 kcal/mol. This value is much lower than the barrier of 53.1 kcal/mol found for the **1OCu** $\rightarrow$ **2OCu** isomerization; therefore, the Cu^+ catalyzed isomerization pathways which originate from **1NCu** may be relevant.

The potential energy curves corresponding to formamide$-Cu^+ \rightarrow$ (aminohydroxy)carbene$-Cu^+$ isomerization processes are given schematically in Figure 4. In this case the primary mechanism is a 1,2H transfer, which connects **1OCu** with **3OCu** through the transient species **TS13OCu** or **1NCu** with **3CCu** through the transition state **TS13NCu**. As before, in the first isomerization process the less stable (aminohydroxy)carbene$-Cu^+$ **3OCu** complex is obtained, so that an internal rotation of its CuOH moiety (through the **TS33** transition state) followed by an OH rotation are required to reach the **3CCu** complex. Once more these internal rotations require much lower energies than the 1,2H transfer involved in the primary mechanism, and therefore the 1,2H transfer becomes the limiting step. The isomerization of **1NCu**, on the contrary, leads directly to the global minimum **3CCu**, since the complex where the metal cation is attached to the amino group of the carbene collapses to the carbon attached structure.

In contrast to what was found before for the formamide $\rightarrow$ formamidic acid isomerization, in this case neither of the two isomerization processes are catalized by Cu^+ association. This is because in the formamide $\rightarrow$ (aminohydroxy)carbene isomerization the 1,2H transfer perturbs significantly the intrinsic basicity of the oxygen atom, which decreases, but perturbs very little that of the amino group, which is not directly involved in the 1,2H transfer. Hence, as in the previous case, it is reasonable to expect the isomerization barrier between **1OCu** and **3OCu** complexes to be higher than that between the corresponding neutrals (see Figure 4). Consistently, the barrier between **1NCu** and **3CCu** should be rather similar to that found between the corresponding neutrals, in agreement with our estimates which show that such a barrier becomes only 2.6 kcal/mol higher upon Cu^+ association (see Figure 4). This result indicates that the amino group of the **TS13** transition state is slightly less basic than the amino group of formamide.

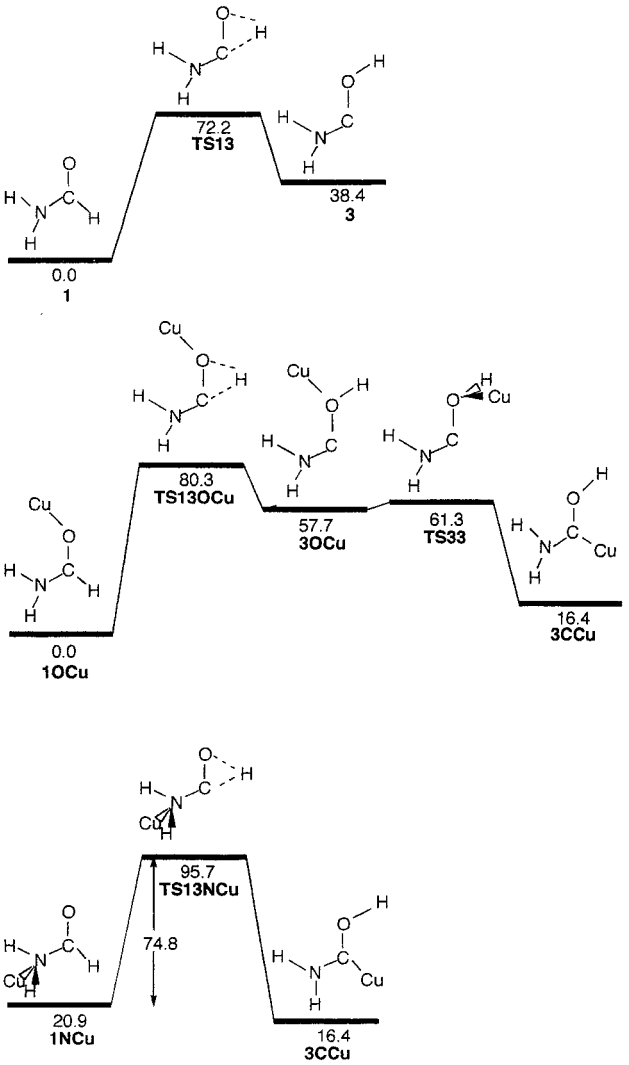

Figure 4. Schematic representation of the PES's associated with the formamide−Cu^+ → (aminohydroxy)carbene−Cu^+ isomerizations. The isomerization between the neutrals is also given for the sake of comparison. Relative energies are in kilocalories per mole.

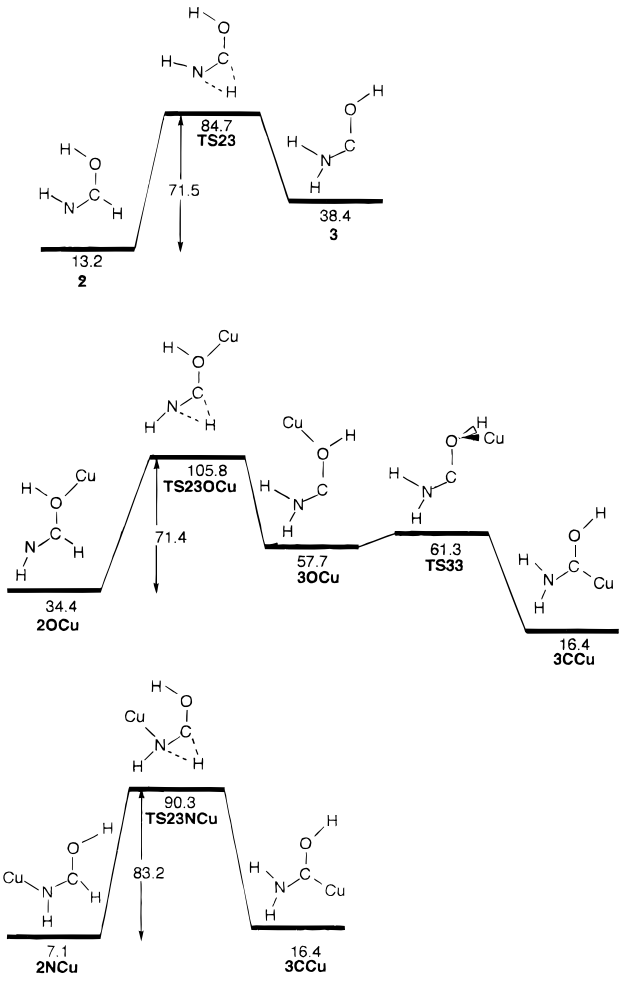

Figure 5. Schematic representation of the PES's associated with the formamidic acid−Cu^+ → (aminohydroxy)carbene−Cu^+ isomerizations. The isomerization between the neutrals is also given for the sake of comparison. Relative energies are in kilocalories per mole.

As before, for the **2** → **3** isomerization reactions two different processes could be envisaged, depending on the center (N or O) to which the metal cation was attached (see Figure 5).

The isomerization pathway which originates with the oxygen attached complex **2OCu** proceeds as a primary mechanism, a 1,2H shift through the transition state **TS23CuO**, which leads to the oxygen attached isomer of the carbene (**3OCu**). A subsequent internal rotation of the CuOH moiety, followed by a rotation of the OH group, yields the carbon attached complex of the carbene (**3CCu**), which is the global minimum. As was found in the previous mechanisms the limiting step is the 1,2H shift which involves an activation barrier much higher than the internal rotations.

Starting from the nitrogen attached complex, **2NCu**, a similar 1,2H shift yields directly the most stable structure, **3CCu**, because the nitrogen attached complex of the (aminohydroxy)-carbene collapses to the carbon attached species.

Following arguments similar to those involved above, a negligible change in the activation barrier between **2OCu** and **3OCu** should be expected in comparison to that between the corresponding neutral species, because the 1,2H transfer does not perturb significantly the intrinsic basicity of the oxygen atom, which is again not directly involved in this process. On the contrary, an anticatalytic effect should be expected, in agreement with our calculated barriers, for the isomerization between **2NCu** and **3CCu** because the intrinsic basicity of the nitrogen atom should decrease as a consequence of the 1,2H transfer.

Conclusions

Similarly to what was found in protonation processes, formamidic acid behaves as a nitrogen base, while (aminohydroxy)carbene behaves as a strong carbon base when the reference acid is Cu^+. More importantly, Cu^+ association leads to a sizable stabilization of both isomers with respect to formamide, which is not observed for other metal monocations such as Li^+, Na^+, Mg^+, or Al^+.

Although both isomers are stabilized by Cu^+ association, the formamide → formamidic acid → (aminohydroxy)carbene isomerization processes are not catalized by Cu^+ ions, since in general the hydrogen transfers involved in the proton transfer processes result in a weakening of the interaction between the neutral and the metal cation. The only exception to this general behavior corresponds to the isomerization between the nitrogen attached formamide complex and the corresponding enolic species, because in this particular case the hydrogen shift involved in the isomerization enhances the ion−neutral interaction.

Acknowledgment. This work has been partially supported by the DGICYT Project No. PB96-0067 and by the Acción Integrada Hispano-Francesa No. HF1996-0184. Generous allocations of computational time at the Centro de Computación Científica de la Facultad de Ciencias de la Universidad Autónoma de Madrid and at the Cray-J90 computer of CIEMAT are also acknowledged. A.L. acknowledges a postdoctoral grant from the EC.

Supporting Information Available: Table of B3LYP/6-311G(d,p) harmonic vibrational frequencies (cm^{-1}) and assignments for **2**, **2NCu**, **3**, and **3CCu** complexes (1 page). See any current masthead page for ordering instructions.

References and Notes

(1) Perrin, C. I. *Acc. Chem. Res.* **1989**, *22*, 286, and references therein.

(2) Antonczak, S.; Ruiz-López, M. F.; Rivail, J. L. *J. Am. Chem. Soc.* **1994**, *116*, 3912, and references cited therein.

(3) McGibbon, G. A.; Burgers, P. C.; Terlouw, J. K. *Int. J. Mass Spectrom. Ion Processes* **1994**, *136*, 191.

(4) Wang, X.; Nichols, J.; Feyereisen, M.; Gutowski, M.; Boatz, J.; Haymet, A. D. J.; Simons, J. *J. Phys. Chem.* **1991**, *95*, 10419.

(5) Wong, M. W.; Wiberg, K. B.; Frisch, M. J. *J. Am. Chem. Soc.* **1992**, *114*, 1645.

(6) Schlegel, H. B.; Ground, P.; Fluder, E. M. *J. Am. Chem. Soc.* **1982**, *104*, 5347.

(7) Kwiatkowski, J. S.; Bartlett, R. J.; Person, W. B. *J. Am. Chem. Soc.* **1988**, *110*, 2353.

(8) Tortajada, J.; Leon, E.; Morizur, J.-P.; Luna, A.; Mó, O.; Yáñez, M. *J. Phys. Chem.* **1995**, *99*, 13890.

(9) Luna, A.; Amekraz, B.; Tortajada, J. *Chem. Phys. Lett.* **1997**, *266*, 31.

(10) Luna, A.; Amekraz, B.; Morizur, J.-P.; Tortajada, J.; Mó, O.; Yáñez, M. *J. Phys. Chem.* **1997**, *101*, 5931.

(11) Luna, A.; Amekraz, B.; Tortajada, J.; Morizur, J.-P.; Alcamí, M.; Mó, O.; Yáñez, M. *J. Am. Chem. Soc.*, in press.

(12) Cerda, B. A.; Wesdemiotis, C. *J. Am. Chem. Soc.* **1995**, *117*, 1734.

(13) Lei, Q. P.; Amster, I. J. *J. Am. Soc. Mass Spectrom.* **1996**, *7*, 722.

(14) Hoyau, S.; Ohanessian, G. *J. Am. Chem. Soc.* **1997**, *119*, 2016.

(15) (a) Wen, D.; Yalcin, T.; Harrison, A. G. *Rapid Commun. Mass Spectrom.* **1995**, *9*, 1155. (b) Lavanant, H.; Hoppilliard, Y. *J. Mass Spectrom.* **1997**, *32*, 1037.

(16) Curtiss, L. A.; Raghavachari, K.; Trucks, G. W.; Pople, J. A. *J. Chem. Phys.* **1991**, *94*, 7221.

(17) Amekraz, B.; Tortajada, J.; Morizur, J.-P.; González, A. I.; Mó, O.; Yáñez, M.; Leito, I.; Maria, P.-C.; Gal, J.-F. *New J. Chem.* **1996**, *20*, 1011.

(18) Smith, B. J.; Radom, L. *J. Am. Chem. Soc.* **1993**, *115*, 4885.

(19) González, A. I.; Mó, O.; Yáñez, M.; León, E.; Tortajada, J.; Morizur, J.-P.; Leito, I.; Maria, P.-C.; Gal, F. *J. Phys. Chem.* **1996**, *100*, 10490.

(20) (a) Becke, A. D. *J. Chem. Phys.* **1993**, *98*, 5648. (b) Becke, A. D. *J. Chem. Phys.* **1992**, *96*, 2155.

(21) Lee, C.; Yang, W.; Parr, R. G. *Phys. Rev.* **1988**, *B37*, 785.

(22) (a) Llamas-Saiz, A. L.; Foces-Foces, C.; Mó, O.; Yáñez, M.; Elguero, E.; Elguero, J. *J. Comput. Chem.* **1995**, *16*, 263. (b) Florián, J.; Johnson, B. G. *J. Phys. Chem.* **1994**, *98*, 3681. (c) Bauschlicher, C. W. *Chem. Phys. Lett.* **1995**, *246*, 40. (d) Martell, J. M.; Goddard, J. D.; Eriksson, L. A. *J. Phys. Chem. A* **1997**, *101*, 1927. (e) Cui, Q.; Musaev, D. G.; Svensson, M.; Sieber, S.; Morokuma, K. *J. Am. Chem. Soc.* **1995**, *117*, 12366. (f) Ricca, A.; Bauschlicher, C. W. *J. Phys. Chem.* **1994**, *98*, 12899. (g) Ricca, A.; Bauschlicher, C. W. *J. Phys. Chem.* **1995**, *99*, 5922. (h) Ricca, A.; Bauschlicher, C. W. *J. Phys. Chem.* **1995**, *99*, 9003. (i) Ziegler, T. *Chem. Rev.* **1991**, *91*, 651.

(23) (a) Watchers, A. J. H. *J. Chem. Phys.* **1970**, *52*, 1033. (b) Hay, P. J. *J. Chem. Phys.* **1977**, *66*, 4377.

(24) Frisch, M. J.; Trucks, G. W.; Schlegel, H. B.; Gill, P. M. W.; Johnson, B. J.; Robb, M. A.; Cheeseman, J. R.; Keith, T. A.; Peterson, G. A.; Montgomery, J. A.; Raghavachari, K.; Al-Laham, M. A.; Zakrzewski, V. G.; Ortiz, J. V.; Foresman, J. B.; Cioslowski, J.; Stefanow, B. B.; Nanayaklara, A.; Challacombe, M.; Peng, C. Y.; Ayala, P. Y.; Chen, W.; Wong, M. W.; Andres, J. L.; Replogle, E. S.; Gomperts, R.; Martin, R. L.; Fox, D. J.; Binkley, J. S.; Defrees, D. J.; Baker, J.; Stewart, J. P.; Head-Gordon, M.; Gonzalez, C.; Pople, J. A. *Gaussian 94*; Gaussian, Inc.: Pittsburgh, PA, 1995.

(25) Bader, R. F. W. *Atoms in Molecules. A Quantum Theory*; Oxford University Press: Oxford, U.K., 1990.

(26) (a) Cremer, D.; Kraka, E. *Chim. Acta* **1984**, *57*, 1529. (b) Cremer, D.; Kraka, E. *Angew. Chem., Int. Ed. Engl.* **1984**, *23*, 627.

(27) The AIMPAC programs package has been provided by J. Cheeseman and R. F. W. Bader.

(28) Alcamí, M.; Mó, O.; Yáñez, M. *J. Phys. Chem.* **1989**, *93*, 3929.

(29) Alcamí, M.; Mó, O.; De Paz, J. L. G.; Yáñez, M. *Theor. Chim. Acta* **1990**, *77*, 1.

(30) Cerda, B. A.; Wesdemiotis, C. *J. Am. Chem. Soc.* **1996**, *118*, 11884.

(31) Alcamí, M.; Mó, O.; Yáñez, M.; Abboud, J.-L. M.; Elguero, J. *Chem. Phys. Lett.* **1990**, *172*, 471.